ACS APPLIED MATERIALS & INTERFACES

Letter

www.acsami.org

Defective Black TiO_2 Synthesized via Anodization for Visible-Light Photocatalysis

Junye Dong,*[,†] Jie Han,[†,‡] Yangsi Liu,[†] Akira Nakajima,[§] Sachiko Matsushita,[§] Shanghai Wei,[†] and Wei Gao[†]

[†]Department of Chemical & Materials Engineering, The University of Auckland, Auckland 1142, New Zealand

[‡]Department of Civil and Environmental Engineering, University of Illinois at Urbana−Champaign, 205 North Mathews Avenue, Urbana, Illinois, United States

[§]Department of Metallurgy & Ceramics Science, Tokyo Institute of Technology, 2-12-1 Ookayama, Meguro-ku, Tokyo 152-8552, Japan

Supporting Information

ABSTRACT: Defective TiO_{2-x} was synthesized via a facile anodization technique. Electron paramagnetic resonance spectra confirmed the presence of oxygen vacancy, which extended the photon-absorbance deeply into the visible-light region. By stripping off the nanotubes on top, a hexagonally dimpled layer of black TiO_{2-x} was exposed and exhibited remarkable photocatalytic activity.

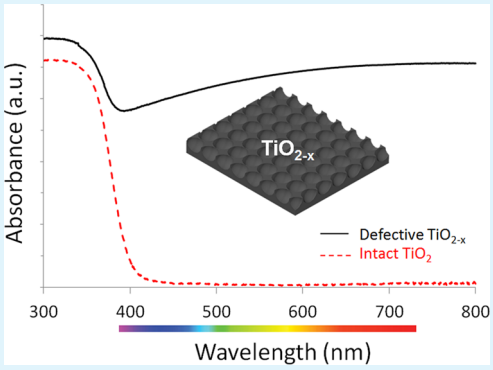

KEYWORDS: *TiO_2, oxygen vacancy, anodization, visible light, photocatalysis*

1. INTRODUCTION

Self-organized titanium dioxide (TiO_2) layer formed by anodization has shown promising applications[1] in water-splitting,[2] photodegradation,[3] sterilization,[4] and solar cells,[5] and attracted substantial research interests for its robust mechanical adhesion and electrical conductivity.[6,7] To promote its light-harvesting capability, attempts have been made to modify anodic TiO_2 nanotubes including, most notably, metal[8] and nonmetal doping.[9,10] An inherent limitation of this approach, however, is that the dopants introduced often acted as charge carrier recombination centers, which compromised the photocatalytic activity of the material.[11]

Recently reported work has shown that, by introducing crystal defects in TiO_2, a new vacancy band could be generated below its conduction band, expanding the photon-absorbance of TiO_2 into the visible light region without the recombination effect from doped impurities.[12−15] Developing a simple and scalable anodization method for the synthesis of defective TiO_2 is therefore of particular interests.[16−18] Herein, we present a facile technique to synthesize oxygen vacancy (V_o)-doped TiO_2 with high visible-light-induced photocatalytic activity. Our experimental evidence highlights a layer of black, deflective anodic TiO_{2-x} that has not been reported in previous studies.

2. EXPERIMENTAL SECTION

By two-step anodization on Ti foil (0.2 mm thick, 99.96%) at 60 V in ethylene glycol containing 0.25 wt.% NH_4F and 2 vol.% distilled water (Scheme 1),[19] a tubular-structured oxide layer was obtained on the Ti substrate after 10 h of anodization. The anodized Ti foil was rinsed in ethanol and distilled water, and dried at 150 °C for completely removing organic species. The cleaned samples were sintered at 450 °C for 1 h in ambient atmosphere. After removing the top oxide layer, an inner layer of black TiO_2 was exposed on the substrate.

3. RESULTS AND DISCUSSION

ESEM images showed the tubular microstructure of the stripped oxide layer on the anodized Ti foil. The internal diameter is estimated to be 150−180 nm at the tip region (Figure 1a), which decreased along the depth direction.[20] The homogeneous structure transformed to double-shelled tubes at the root segment after annealing, with the inner shell composed of nanoparticles (see Figure S1 in the Supporting Information). These nanotubes are approximately 115 μm in length, giving a draw ratio of more than 660 (see Figure S2 in the Supporting

Received: December 3, 2013
Accepted: January 27, 2014
Published: February 4, 2014

Scheme 1. Experimental Process and Optical Images of the Stripped TiO_2 Layer

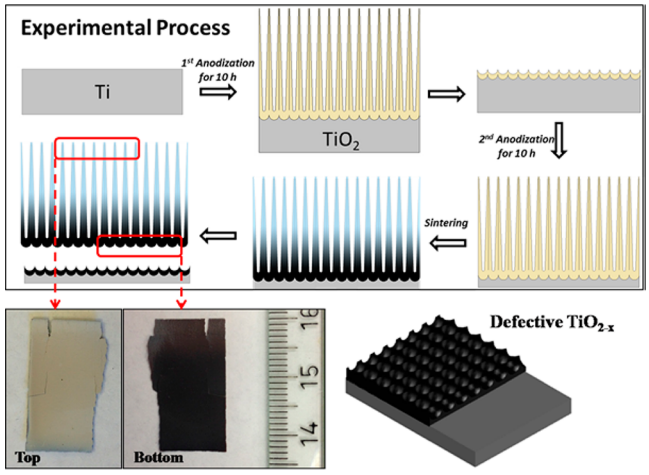

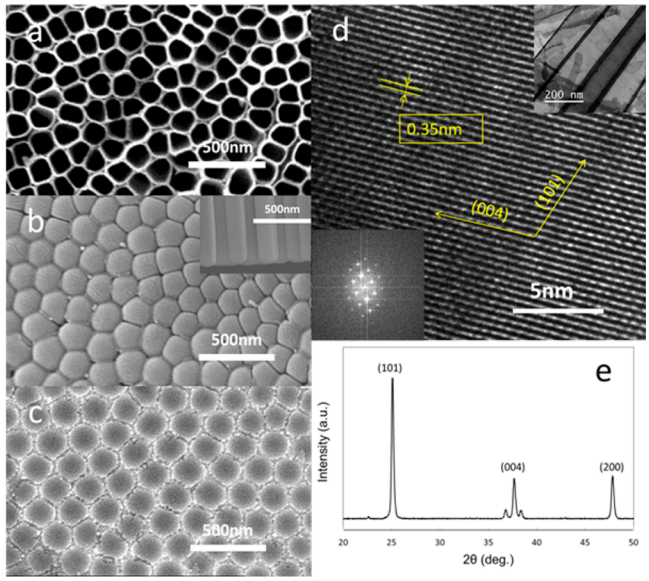

Figure 1. Morphologies of the anodized TiO_2 nanotubes and black TiO_2 layer: (a) Top view, (b) bottom view of TiO_2 nanotubes, and (c) the black TiO_2 layer covered on Ti substrate after stripping off the nanotubes grown on top. (d) HRTEM images and (e) XRD analysis of the anodized TiO_2.

Information). The bottom of these nanotubes exhibits a hexagonal topography (Figure 1b). Detailed topographies of the root segment are shown in the insets of Figures 1b. By removing these nanotubes on top, a black oxide layer was exposed which covered the Ti substrate with a hexagonally dimpled morphology (Figure 1c).[21]

HRTEM micrograph and X-ray diffraction show that the anodic TiO_2 was in pure anatase phase (Figure 1d, e), and exhibited nanocrystal with the characteristic disorder surface layer (see Figure S3 in the Supporting Information). EDX results verified the incorporation of fluorine ion (F^-) in the as-prepared Ti substrate, which vanished after sintering (see Figure S4 in the Supporting Information). The electron paramagnetic resonance (EPR) spectrum recorded at room temperature confirmed the significant presence of V_o in the black TiO_2, with a strong signal at $g = 2.003$ induced by electrons trapped on V_o (Figure 2).[22−24] Such signal was not observed in the EPR spectrum of commercial P25 TiO_2 (see Figure S5 in the Supporting Information). The EPR spectra also indicate that there was no Ti^{3+} present in the black TiO_2, as characterized by the absence of the signal at $g = 1.975$.[17]

Approximately 73% V_o in anodic TiO_{2-x} was consumed after directly sintering in a preheated furnace (Figure 2a). More V_o was consumed after sintering in a cold furnace, which was heated from room temperature to 450 °C. (Figure 2b). It is interesting to find that the concentration of oxygen-vacancy $C(V_o)$ kept constant after annealing for different time or with different heating speeds (Figure 2c, d). This might be ascribed to the presence of initially formed crystalline layer outside, which prevented the inside V_o from oxidation by O_2 in air.

The presence of V_o in anodized TiO_{2-x} can be explained by the oxide formation mechanisms. During anodization, the formation of TiO_2 is a dynamic process involving oxidation at the oxide/metal interface and chemical dissolution at the oxide/electrolyte interface.[23] In oxidation process, water molecules from the electrolyte solution acted as the oxygen source. The diffusion of electroneutral water molecules was quite difficult, hindered by the large draw ratio of these nanotubes grown on top.,[25,26] As a result, the oxidation process suffered from the insufficient supply of oxygen.[27] V_o and Ti^{3+} might be produced simultaneously at the oxide/metal interface. At the same time, negatively charged F^- ion were attracted to the anode by electrical field, and consumed the generated Ti^{3+} ions as they were more active and vulnerable to chemical dissolution. Therefore, a defective, nonstoichiometric titanium oxide (TiO_{2-x}) layer was formed on the Ti substrate with rich oxygen vacancies.

Infrared spectroscopy analysis shows no difference in anodic TiO_{2-x} chemical structure compared to the intact TiO_2 (Figure 3a). However, the diffuse reflectance UV−vis spectrum of TiO_{2-x} exhibited ultrahigh absorbance over the full visible light region (400−800 nm), twice as the absorbance of previously reported TiO_{2-x}, which was reduced by H_2 (HP-TiO_{2-x}) (Figure 3b).[28] A steep increase in light absorbance is observed in all samples at wavelengths below 400 nm, the photon absorbance of TiO_{2-x} significantly extends into longer wavelengths, maintaining a high level of absorbance through the entire visible light region. The black TiO_{2-x} layer also showed dramatically higher visible-light absorbance than the tubular TiO_2 grown on top (see Figure S6 in the Supporting Information).

Photocatalytic activity of the anodic black TiO_{2-x} was assessed by monitoring the degradation of Rhodamine B (RhB, a model organic dye) in water under blue light irradiation (400−500 nm) (Figure 3c). TiO_{2-x}, which sintered in a preheated furnace containing high $C(V_o)$, initiated rapid degradation of RhB in water, with ~80% RhB degraded after 4 h irradiation. In contrast, TiO_{2-x} of low $C(V_o)$ degraded ~60% RhB within 4 h. It shows that high $C(V_o)$ could strengthen the photocatalytic properties under visible light. The photocatalytic result, that the postannealed TiO_{2-x} failed to reduce RhB, confirmed the above hypothesis: V_o was exposed after removing the top oxide layer and existed on TiO_2 surface.

TiO_2 nanotubes, which have a larger surface area as shown in the ESEM images, enabled much slower degradation of the model dye. Due to its hexagonally dimpled morphology, the black TiO_{2-x} has a relatively small surface area compared to the TiO_2 nanotubes. However, its remarkable photocatalytic activity proved it to be as an excellent photocatalyst under visible light. In addition, its robust nonporous structure and immobilized nature may be further exploited to overcome issues of photocatalyst

dx.doi.org/10.1021/am405549p | ACS Appl. Mater. Interfaces 2014, 6, 1385−1388

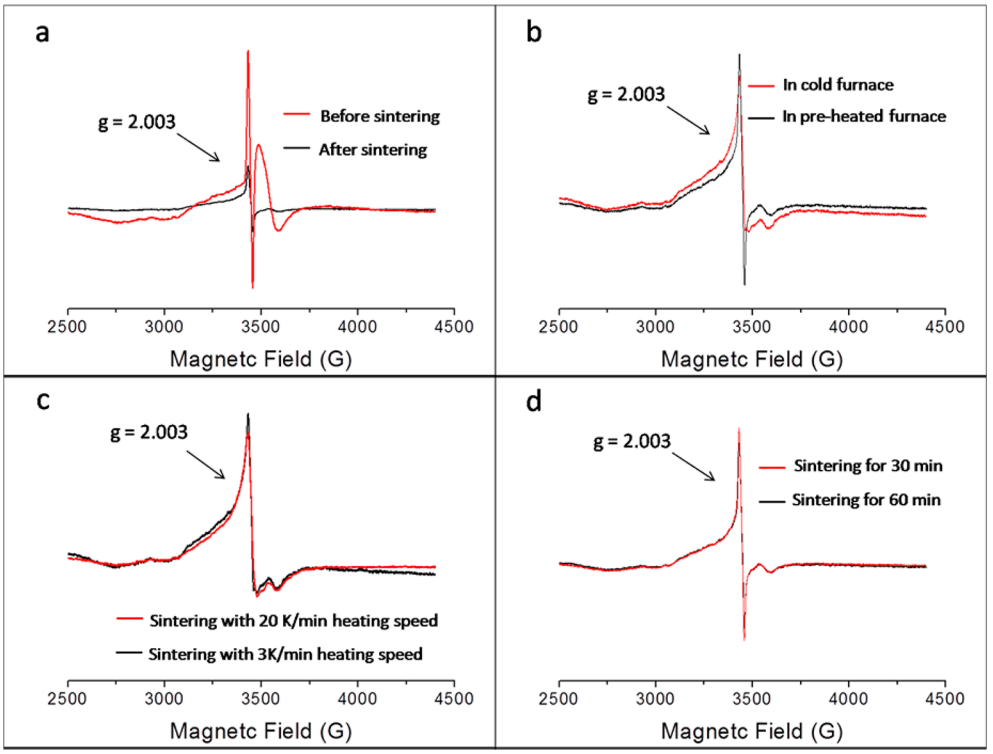

Figure 2. EPR spectra of the anodic TiO_{2-x} with different heat treatments: (a) before/after sintering; (b) sintering by putting sample in a preheated furnace/cold furnace which was heated from room temperature; (c) sintering in a cold furnace with 3 K/20 K heating speeds; (d) sintering in a preheated furnace for 30 min/60 min.

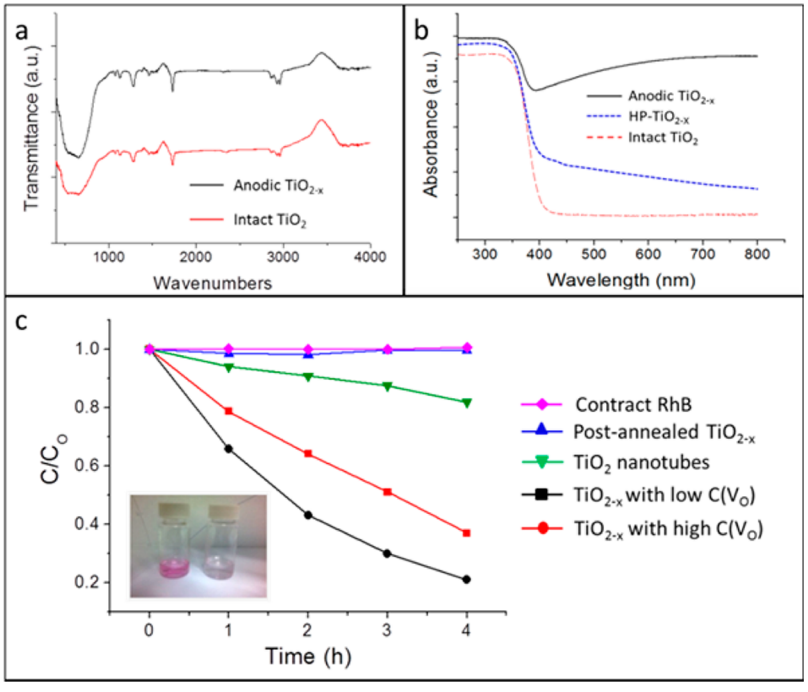

Figure 3. (a) Infrared spectrum of anodic TiO_{2-x} and intact TiO_2. (b) Diffuse reflectance UV−vis spectrum of anodic TiO_{2-x}, high-pressure hydrogenated black titania (HP−TiO_2),[28] and intact TiO_2. (c) Photocatalytic degradation of RhB under blue light (400−500 nm) irradiation.

recovery that prove to be difficult with fine particles or thin whiskers photocatalyst.

4. CONCLUSIONS

In conclusion, the present work demonstrates a facile anodization technique to synthesize defective black TiO_2 with controllable level of defects, which exhibited high photocatalytic activity under visible light. Mechanistic analysis and characterization results indicate that oxygen vacancies were formed in an oxygen-deficient environment during the anodization process and account for the high photon-absorbance of the black TiO_{2-x} throughout the visible-light region.

dx.doi.org/10.1021/am405549p | ACS Appl. Mater. Interfaces 2014, 6, 1385−1388

■ ASSOCIATED CONTENT

Supporting Information

Detailed experimental procedures, HRTEM and ESEM images of anodized TiO_2, EDX spectra of the anodized Ti substrate, EPR spectra of anodized TiO_2 and P25, diffusion reflectance UV−vis absorption spectra of anodic TiO_2 nanotubes. This material is available free of charge via the Internet at http://pubs.acs.org

■ AUTHOR INFORMATION

Corresponding Author

*E-mail: jdon853@aucklanduni.ac.nz. Phone: + 64 (0) 211931953.

Notes

The authors declare no competing financial interest.

■ ACKNOWLEDGMENTS

The authors thank the group and Department members for their assistances.

■ REFERENCES

(1) Macak, J. M.; Tsuchiya, H.; Taveira, L.; Aldabergerova, S.; Schmuki, P. *Angew. Chem., Int. Ed.* **2005**, *44*, 7463−7465.
(2) Park, J. H.; Kim, S.; Bard, A. J. *Angew. Chem., Int. Ed.* **2005**, *6*, 24−28.
(3) He, X.; Cai, Y.; Zhang, H.; Liang, C. *J. Mater. Chem.* **2011**, *21*, 475−480.
(4) Guin, D.; Manorama, S. V.; Latha, J. N. L.; Singh, S. *J. Phys. Chem. C* **2007**, *111*, 13393−13397.
(5) Zhu, K.; Neale, N. R.; Miedaner, A.; Frank, A. J. *Nano Lett.* **2006**, *7*, 69−74.
(6) Hirakata, H.; Ito, K.; Yonezu, A.; Tsuchiya, H.; Fujimoto, S.; Minoshima, K. *Acta Mater.* **2010**, *58*, 4956−4967.
(7) El Ruby Mohamed, A.; Rohani, S. *Energy Environ. Sci.* **2011**, *4*, 1065−1086.
(8) Hoffmann, M. R.; Martin, S. T.; Choi, W.; Bahnemann, D. W.; Bahnemann, D. W. *Chem. Rev.* **1995**, *95*, 69−96.
(9) Khan, S. U. M.; Al-Shahry, M.; Ingler, W. B. *Science* **2002**, *297*, 2243−2245.
(10) Asahi, R.; Morikawa, T.; Ohwaki, T.; Aoki, K.; Taga, Y. *Science* **2001**, *293*, 269−271.
(11) Choi, W.; Termin, A.; Hoffmann, M. R. *J. Phys. Chem.* **1994**, *98*, 13669−13679.
(12) Leshuk, T.; Parviz, R.; Everett, P.; Krishnakumar, H.; Varin, R. A.; Gu, F. *ACS Appl. Mater. Interfaces* **2013**, *5*, 1892−1895.
(13) Yoshitake, H.; Sugihara, T.; Tatsumi, T. *Chem. Mater.* **2002**, *14*, 1023−1029.
(14) Naldoni, A.; Allieta, M.; Santangelo, S.; Marelli, M.; Fabbri, F.; Cappelli, S.; Bianchi, C. L.; Psaro, R.; Dal Santo, V. *J. Am. Chem. Soc.* **2012**, *134*, 7600−7603.
(15) Jiang, X.; Zhang, Y.; Jiang, J.; Rong, Y.; Wang, Y.; Wu, Y.; Pan, C. *J. Phys. Chem. C* **2012**, *116*, 22619−22624.
(16) Wang, Z.; Yang, C.; Lin, T.; Yin, H.; Chen, P.; Wan, D.; Xu, F.; Huang, F.; Lin, J.; Xie, X.; Jiang, M. *Adv. Funct. Mater.* **2013**, *23*, 5444−5450.
(17) Zuo, F.; Wang, L.; Wu, T.; Zhang, Z.; Borchardt, D.; Feng, P. *J. Am. Chem. Soc.* **2010**, *132*, 11856−11857.
(18) Naldoni, A.; Allieta, M.; Santangelo, S.; Marelli, M.; Fabbri, F.; Cappelli, S.; Bianchi, C. L.; Psaro, R.; Dal Santo, V. *J. Am. Chem. Soc.* **2012**, *134*, 7600−7603.
(19)
(20) Dong, J.; Han, J.; Qiu, W.; Huang, S.; Gao, W. *Scr. Mater.* **2013**, *69*, 374−376.
(21) Zhang, G.; Huang, H.; Zhang, Y.; Chan, H. L. W.; Zhou, L. *Electrochem. Commun.* **2007**, *9*, 2854−2858.
(22) Randorn, C.; Irvine, J. T. S. J. *Mater. Chem.* **2010**, *20*, 8700−8704.
(23) Prokes, S. M.; Gole, J. L.; Chen, X.; Burda, C.; Carlos, W. E. *Adv. Funct. Mater.* **2005**, *15*, 161−167.
(24) Naldoni, A.; D'Arienzo, M.; Altomare, M.; Marelli, M.; Scotti, R.; Morazzoni, F.; Selli, E.; Dal Santo, V. *Appl. Catal., B* **2013**, *130*, 239−248.
(25) Prakasam, H. E.; Shankar, K.; Paulose, M.; Varghese, O. K.; Grimes, C. A. *J. Phys. Chem. C* **2007**, *111*, 7235−7241.
(26) Paulose, M.; Shankar, K.; Yoriya, S.; Prakasam, H. E.; Varghese, O. K.; Mor, G. K.; Latempa, T. A.; Fitzgerald, A.; Grimes, C. *J. Phys. Chem. B* **2006**, *110*, 16179−16184.
(27) Chen, C. C.; Say, W.; Hsieh, S. J.; Diau, E. *Appl. Phys. A: Mater. Sci. Process.* **2009**, *95*, 889−898.
(28) Chen, X.; Liu, L.; Yu, P. Y.; Mao, S. S. *Science* **2011**, *331*, 746−750.